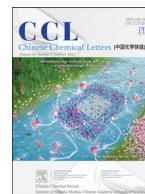Contents lists available at ScienceDirect

Chinese Chemical Letters

journal homepage: www.elsevier.com/locate/cclet

Mechanochemical transformation of fluorescent hydrogel based on dynamic lanthanide-terpyridine coordination

Guangqiang Yin [a,b,c], Jianxiang Huang [d], Depeng Liu [b,c], Rui Li [b,c], Shuxin Wei [b,c], Muqing Si [b,c], Feng Ni [b,c], Yinfei Zheng [a,e,*], Qiu Yang [f], Ruhong Zhou [d,*], Xiaoxia Le [b,c,*], Wei Lu [b,c], Tao Chen [b,c,*]

[a] *Key Laboratory for Biomedical Engineering of Ministry of Education Ministry of China, College of Biomedical Engineering and Instrument Science, Zhejiang University, Hangzhou 310027, China*
[b] *Key Laboratory of Marine Materials and Related Technologies, Zhejiang Key Laboratory of Marine Materials and Protective Technologies, Ningbo Institute of Materials Technology and Engineering, Chinese Academy of Sciences, Ningbo 315201, China*
[c] *School of Chemical Sciences, University of Chinese Academy of Sciences, Beijing 100049, China*
[d] *Institute of Quantitative Biology, Zhejiang University, Hangzhou 310027, China*
[e] *Research Center for Intelligent Sensing, Zhejiang Lab, Hangzhou 311100, China*
[f] *Ningbo New Material Testing and Evaluation Center Co., Ltd., Ningbo 315000, China*

ARTICLE INFO

ABSTRACT

As a burgeoning research field, ultrasound-responsive materials have attracted intense interest in healthcare research. However, the basic mechanism of sonochemical effect in the *quasi*-solid state is far from being well understood than those in the solution. Herein, we showcase mechanochemical transformations of europium(III) complexes in a supramolecular hydrogel matrix. With the combination of labile terpyridine-europium complexes (TPY-Eu^{3+}) as mechanochromic moieties and an ultrasound-responsive fluorogen (URF) as a molecular tweezer, the hydrogel produces a notable fluorescence change in response to ultrasound. The mechanochemical transformation was elucidated by molecular dynamics (MD) simulations, and fully probed and evidenced by electrochemical experiments, X-ray photoelectron spectroscopy (XPS), and attenuated total reflectance-Fourier transform infrared (ATR-FTIR) spectroscopy.

© 2023 Published by Elsevier B.V. on behalf of Chinese Chemical Society and Institute of Materia Medica, Chinese Academy of Medical Sciences.

In recent years, a myriad of organic and inorganic smart materials has been created to sense ultrasound, with enormous applications in navigation, diagnosis, imaging, and so on [1–5]. Among these ultrasound-responsive materials, mechanochromic polymers based on mechanophores exhibit an excellent capacity to change their photophysical properties upon exposure to ultrasound in solution, which has recently fascinated chemists due to their versatile designs and potential applications [6–12]. However, the activation of these covalent-bond-scission-based mechanochromic polymers preferably occurs in the solution state under an acoustic field, thus severely limiting their practical utilization. Differently, the supramolecular metal-ligand (M-L) complex as a dynamic mechanochromic moiety makes it possible to realize a highly reversible and sensitive response to ultrasound in the *quasi*-solid state with relatively lower acoustic energy [13–19].

Hydrogels are an attractive class of intelligent materials due to their highly water-swollen *quasi*-solid feature, exhibiting unique properties of both solid and liquid, including intrinsic soft and wet nature, multistimulus responsiveness [20–43]. By virtue of these merits, the dynamic hydrogels offer an ideal platform to develop ultrasound-responsive materials by incorporating reversible M-L interactions. Importantly, it may provide new insights into sonochemical effects to advance the understanding of mechanochemical transformation in the *quasi*-solid [44]. Compared with those polymers that can only respond in the solution, the ultrasound-responsive hydrogels hold great promise in diverse biomedical applications including diagnosis, imaging, and biosensing.

Herein, we report a feasible strategy to fabricate ultrasound-responsive supramolecular hydrogels through the combination of labile terpyridine-europium complex (TPY-Eu^{3+}) as a mechanochromic moiety and an ultrasound-responsive fluorogen (URF) as a molecular tweezer (Scheme 1). In the fabrication process of ultrasound-responsive hydrogels, firstly, the terpyridine-functionalized monomer TPY-M was synthesized through two steps of nucleophilic substitution reactions in decent yields (Scheme S1
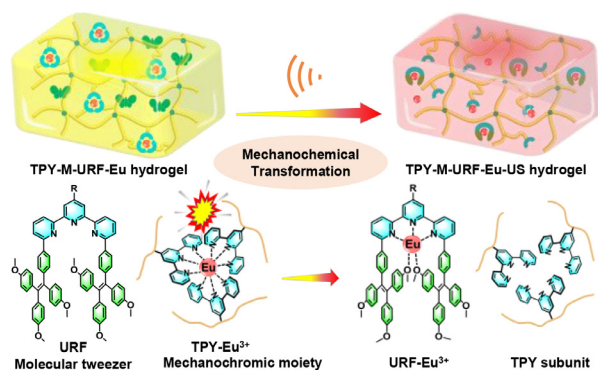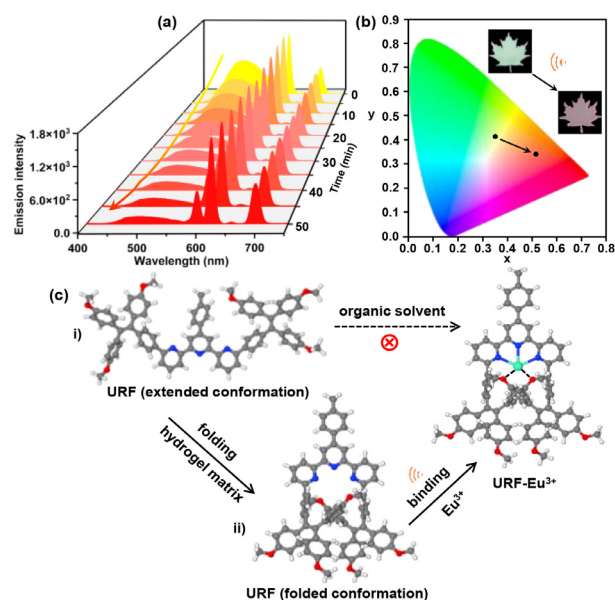
Scheme 1. Illustration of the mechanochemical transformation of europium(III) complexes in the TPY-M-URF-Eu hydrogel matrix upon the irradiation of ultrasound.

Fig. 1. (a) Fluorescence spectra of TPY-M-URF-Eu hydrogel upon exposure to ultrasound, $\lambda_{ex} = 254$ nm. (b) Fluorescent color changes at a CIE (1931) coordinate diagram. Inset: photographs of TPY-M-URF-Eu hydrogel, TPY-M-URF-Eu-US hydrogel under 254 nm light. (c) Mechanochemical assembly of URF-Eu^{3+} complex, geometrically optimized structures of URF (i: extended conformation in organic solvents, ii: folded conformation in hydrogel matrix) and URF-Eu^{3+} complex.

in Supporting information). The hydrophobic URF was synthesized by introducing two tetraphenylethylene (TPE) groups onto the 6,6″ position of TPY core through Suzuki coupling as outlined in Scheme S2 (Supporting information). The TPE groups on URF not only serve as luminophores to guarantee the efficient emission based on aggregation-induced emission (AIE) [45–53], but also act as bulky groups to inhibit coordination without the assistance of ultrasound in the hydrogel matrix. Both TPY-M and URF were completely verified by nuclear magnetic resonance (NMR), including ^{1}H, ^{13}C, two-dimensional correlation spectroscopy (2D-COZY), nuclear Overhauser effect spectroscopy (2D-NOESY), high-resolution electrospray ionization time-of-flight (ESI-TOF) mass spectrometer (Figs. S1-S8, S10 and S11 in Supporting information).

Subsequently, TPY-M hydrogel was prepared by free-radical copolymerization of acrylamide (AAm), TPY-M, methylene bisacrylamide (MBAA) crosslinker, using AIBN as the thermal initiator in DMSO, followed by the solvent exchange in deionized water (Scheme S3 in Supporting information). The ultrasound-responsive hydrogel TPY-M-Eu was prepared by immersing TPY-M hydrogel into a solution of Eu(NO$_3$)$_3$ at room temperature. Likewise, ultrasound-responsive hydrogel TPY-M-URF-Eu was prepared by incorporating URF into the chemically crosslinked polymer network, followed by solvent exchange and coordination (see Supporting information for details). The chemical structures and compositions of hydrogels were thoroughly investigated by attenuated total reflectance-Fourier transform infrared (ATR-FTIR) spectroscopy (Fig. S20 in Supporting information) and X-ray photoelectron spectroscopy (XPS) experiments (Fig. S22 in Supporting information).

We reasoned that through introducing AIE luminogens (AIEgen), the hydrogels would exhibit remarkable emission efficiency. Indeed, as displayed in Fig. S14 (Supporting information), the TPY-M-URF hydrogel emits intense green fluorescence (centered at *ca.* 500 nm). Particularly, the emission of TPY-M-URF-Eu hydrogel displays strong yellowish fluorescent color, which is the overlapping luminescence of the URF and TPY-Eu^{3+} coordination complex. The fluorescent spectrum of TPY-M-URF-Eu hydrogel reveals two main parts centered at around 500 nm from URF, 590 nm, 615 nm and 690 nm attributed to the TPY-Eu^{3+} complex [15,54], respectively. It indicates that no coordination occurs spontaneously between URF and Eu^{3+}. Ultraviolet−visible (UV−vis) titration and NMR experiments also demonstrate that URF is unable to bind with Eu^{3+} in organic solvents even under sonication (Figs. S9 and S12 in Supporting information).

However, upon the irradiation of ultrasound, the emission band centered at *ca.* 500 nm was decreased over time, indicating that URF was consecutively coordinated with Eu^{3+} ions in the matrix of TPY-M-URF-Eu hydrogel (Fig. 1a). It is reflected in a decrease of the I_{500}/I_{615} ratio (Fig. S15 in Supporting information). The I_{500}/I_{615}

fluorescent ratio decreased dramatically from 0.58 to 0.30 in the initial 10 mins and reached a plateau after *ca.* 40 min. It resulted in obvious fluorescence color-changing from bright yellowish (0.35, 0.44) to orange (0.52, 0.37) at the 1931 Commission Internationale de L'Eclairage (CIE) chromaticity diagram (Fig. 1b). Similarly, the emission intensity of TPY-M-Eu hydrogel underwent a considerable decrease upon sonication owing to the dissociation of TPY-Eu^{3+} assembly [16]. These results manifested that ultrasound-responsive hydrogels presented excellent color changes when subjected to ultrasonic irradiation, and also suggested the mechanochemical transformation taking place in the hydrogel matrix.

It was proposed that the dynamic TPY-Eu^{3+} complex was disassembled along with releasing of URF from aggregation, followed by the formation of a more stable URF-Eu^{3+} assembly when TPY-M-URF-Eu hydrogel was subjected to ultrasonic irradiation (Fig. 1c) [55]. Compared with the conformation in the organic solvents, the energy-minimized structure of URF preferably adopted a folded conformation in the hydrogel matrix. Thus, URF was capable of capturing Eu^{3+} like a molecular tweezer to form a stable supramolecular assembly. Subsequently, the URF-Eu^{3+} assembly might be further stabilized by the residual groups of polymer chains in the hydrogel network. After coordination, the URF served as a UV absorbing ligand to enable the emission of Eu(III) through a ligand-to-metal energy-transfer process, *i.e.*, "antenna effect" [56].
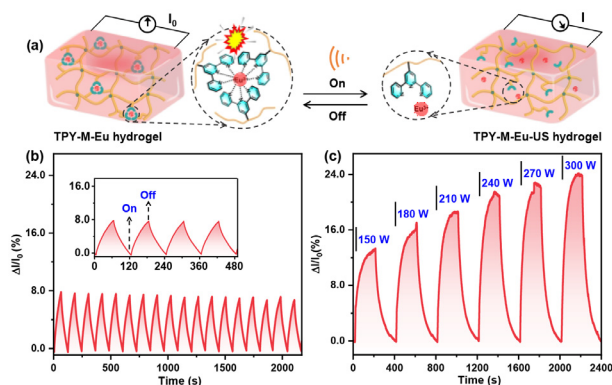
To further investigate the structural conformations of URF and TPY subunit in the hydrogel matrix, molecular dynamics (MD) simulations were further conducted by using the two torsion angles (N-C-C-N) as collective variables (Fig. 2 and Fig. S24 in Supporting information). Intriguingly, the free energy landscape of TPY subunit is highly symmetrical with a free energy barrier of ~20 kJ/mol (Fig. 2a), while the free energy landscape of URF is less symmetrical with a much higher free energy barrier of ~90 kJ/mol (Fig. 2b). It implies that the conformational space of URF is more confined to bind with Eu^{3+} due to the bulky size of TPE groups. The free energy profile along one dihedral is shown in Fig. 2c. Both the free energy minimum of the TPY subunit and URF have small dihedral
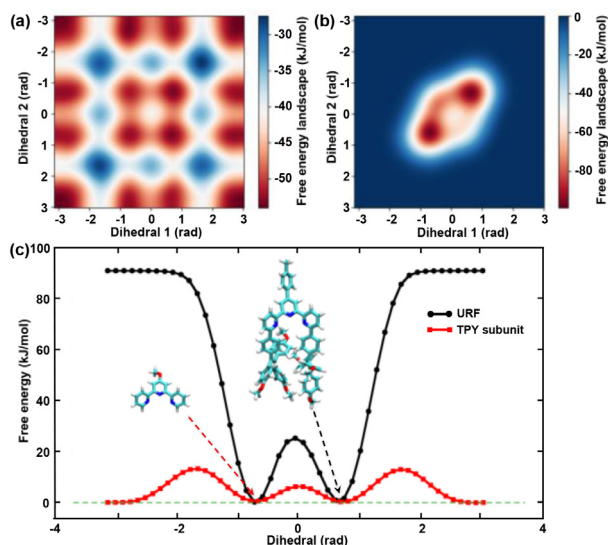
Fig. 2. Two-dimensional free energy landscape of (a) TPY subunit and (b) URF in the hydrogel matrix. (c) One-dimensional free energy of TPY subunit and URF with the representative structures of free energy minimum shown in the inset.

angles with the three nitrogen atoms close to each other (inset of Fig. 2c). It also demonstrates that the optimized structure of URF in the hydrogel matrix is prone to adopt a folded conformation due to its hydrophobic feature. The calculated binding energies of Eu^{3+} with URF and TPY subunit are -48.52 eV and -41.26 eV, respectively. Prominently, it will be more difficult for Eu^{3+} to extricate from URF entrapment than the TPY subunit if hydrophilic and hydrophobic factors are taken into account. That is probably why the coordination bonds of TPY-Eu^{3+} were disrupted while the supramolecular URF-Eu^{3+} complex was assembled simultaneously in the hydrogel matrix upon the irradiation of ultrasound. The MD simulation and theoretical calculation demonstrate that the fluorescence response of TPY-M-URF-Eu hydrogel results from the mechanochemical transformation of europium(III) complexes.

To gain more insights into the mechanism of sonochemical effect, electrochemical experiments were performed to probe the dissociation of the labile TPY-Eu^{3+} complex upon sonication (Fig. 3a). The output signal intensity of the relative current change $\Delta I/I_0$ was consecutively increased to 7.8% when the TPY-M-Eu hydrogel was subjected to ultrasonic irradiation (Fig. 3b). It sug-
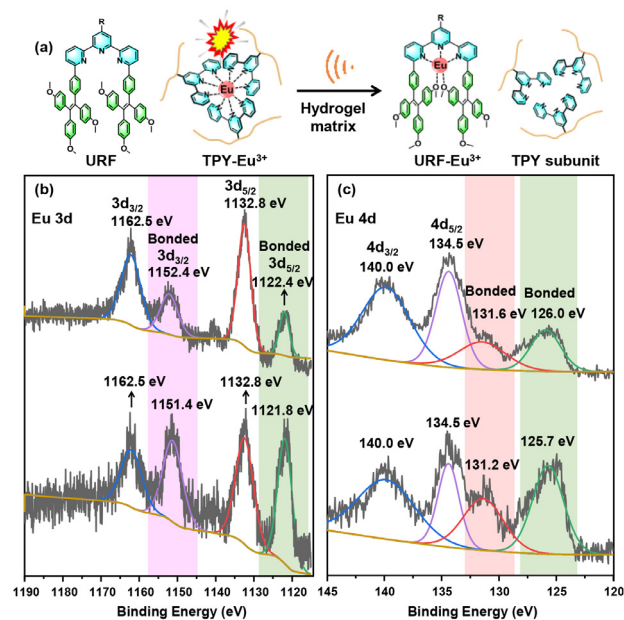
gested that the mobile europium ions were increased under acoustic cavitation owing to the disassembly of the TPY-Eu^{3+} complex. The relative current returned to its initial value gradually at an ultrasound-free state because of the rebinding of the coordination bonds. Notably, the relative current was further increased with the increment of ultrasonic power (from 150 W to 300 W) and longer duration (200 s) as shown in Fig. 3c, indicating that the extent of disassembly could be tuned by varying acoustic energy and duration. To verify the role of the weak coordination bonds, the TPY-M hydrogel served as a control. By comparison, there was no significant change of output current when TPY-M hydrogel was subjected to ultrasonic irradiation (Fig. S23 in Supporting information). These results manifested that the dynamic coordination bonds of TPY-Eu^{3+} were dissociated at an acoustic field so that there were more mobile Eu^{3+} in the hydrogel matrix, leading to the increases of current.

Moreover, XPS experiments were carried out to study the sonochemical transformation of europium(III) complexes in TPY-M-URF-Eu hydrogel at an acoustic field (Fig. 4a). After sonication, the intensity of peaks at around 1151.4 eV (Eu $3d_{3/2}$) and 1121.8 eV (Eu $3d_{5/2}$) for TPY-M-URF-Eu-US hydrogel were blueshifted from 1152.4 eV and 1122.4 eV for TPY-M-URF-Eu hydrogel, respectively, due to the coordination of the URF with Eu^{3+} (Fig. 4b). Also, because of the stronger electron-donating ability of URF than TPY subunit, downshifts of Eu $4d_{3/2}$ and Eu $4d_{5/2}$ from 131.6 eV and 126.0 eV for TPY-M-URF-Eu hydrogel to 131.2 eV and 125.7 eV, respectively, for TPY-M-URF-Eu-US hydrogel, indicating the formation of URF-Eu^{3+} assembly (Fig. 4c). Additionally, the transformation of europium(III) complexes upon sonication were further investigated by ATR-FTIR spectroscopy. As revealed in Fig. S21 (Supporting information), the stretching vibrations of pyridine ring (C=N, C=C) moved from 1600.6 cm^{-1} for TPY-M-URF-Eu hydrogel to 1598.6 cm^{-1} for TPY-M-URF-Eu-US hydrogel. These results confirmed that the URF-Eu^{3+} complex was assembled in the hydrogel matrix upon ultrasound irradiation, leading to visible fluorescence color-changing.

In summary, our study provides new prospects for fabricating ultrasound-responsive hydrogel materials *via* the combination of supramolecular labile TPY-Eu^{3+} bonds and URF, where the TPY-

Fig. 3. (a) Schematic illustration of monitoring the dissociation of TPY-Eu^{3+} complex in the TPY-M-Eu hydrogel matrix upon ultrasound stimulus. (b) The relative current variation of the TPY-M-Eu hydrogel by applying alternating sonication (150 W, 40 kHz) with 60 s intervals. Inset: Enlarged signals of the relative current variation in the 1st–4th cycles. (c) The relative current variation of the TPY-M-Eu hydrogel by applying alternating sonication (150–300 W, 40 kHz) with 200 s intervals.

Fig. 4. (a) The dissociation of TPY-Eu^{3+} and assembly of URF-Eu^{3+} upon sonication in the hydrogel matrix. High-resolution of (b) Eu 3d and (c) Eu 4d XPS spectra of TPY-M-URF-Eu hydrogel (top), and TPY-M-URF-Eu-US hydrogel (bottom).

Eu^{3+} complex servers as mechanochromic moiety and europium ion source, and URF acts like a molecular tweezer to capture mobile Eu^{3+}. The disassembly of TPY-Eu^{3+} complexes and the formation of supramolecular URF-Eu^{3+} assembly leads to a notable fluorescence change in response to ultrasound. The mechanochemical transformation of europium(III) complexes in hydrogel matrix have been demonstrated by MD simulations and evidenced by electrochemical experiments, XPS and ATR-FTIR. The ultrasound-responsive hydrogel materials are expected to possess a broad potential for applications in ultrasound diagnosis, imaging, and so on.

Declaration of competing interest

Supplementary materials

Supplementary material associated with this article can be found, in the online version, at doi:10.1016/j.cclet.2022.03.013.

References

[1] R. Shnaiderman, G. Wissmeyer, O. Ülgen, et al., Nature 585 (2020) 372–378.
[2] X. Wang, X. Yu, X. Wang, et al., Nano Lett. 19 (2019) 2251–2258.
[3] Y. Zhong, Y. Zhang, J. Xu, et al., ACS Nano 13 (2019) 3387–3403.
[4] A.G. Athanassiadis, Z. Ma, N. Moreno-Gomez, et al., Chem. Rev. 122 (2022) 5165–5208.
[5] H. Liu, X. Xiang, J. Huang, et al., Chin. Chem. Lett. 32 (2021) 1759–1764.
[6] G. Cravotto, E.C. Gaudino, P. Cintas, Chem. Soc. Rev. 42 (2013) 7521–7534.
[7] Y. Chen, G. Mellot, D. van Luijk, C. Creton, R.P. Sijbesma, Chem. Soc. Rev. 50 (2021) 4100–4140.
[8] M.E. McFadden, M.J. Robb, J. Am. Chem. Soc. 141 (2019) 11388–11392.
[9] Y. Zhou, S. Huo, M. Loznik, et al., Angew. Chem. Int. Ed. 60 (2021) 1493–1497.
[10] J. Yang, M. Horst, S.H. Werby, et al., J. Am. Chem. Soc. 142 (2020) 14619–14626.
[11] H. Zhang, X. Li, Y. Lin, et al., Nat. Commun. 8 (2017) 1147.
[12] R. Nixon, G. De Bo, Nat. Chem. 12 (2020) 826–831.
[13] J.B. Beck, S.J. Rowan, J. Am. Chem. Soc. 125 (2003) 13922–13923.
[14] W. Weng, J.B. Beck, A.M. Jamieson, S.J. Rowan, J. Am. Chem. Soc. 128 (2006) 11663–11672.
[15] P. Chen, Q. Li, S. Grindy, N. Holten-Andersen, J. Am. Chem. Soc. 137 (2015) 11590–11593.
[16] D.W.R. Balkenende, S. Coulibaly, S. Balog, et al., J. Am. Chem. Soc. 136 (2014) 10493–10498.
[17] G.A. Filonenko, J.A.M. Lugger, C. Liu, et al., Angew. Chem. Int. Ed. 57 (2018) 16385–16390.
[18] B. Liang, R. Tong, Z. Wang, S. Guo, H. Xia, Langmuir 30 (2014) 9524–9532.
[19] S. Cheng, Z. Chen, Y. Yin, Y. Sun, S. Liu, Chin. Chem. Lett. 32 (2021) 3718–3732.
[20] T. Matsuda, R. Kawakami, R. Namba, T. Nakajima, P.G. Jian, Science 363 (2019) 504–508.
[21] H. Yang, C. Li, M. Yang, et al., Adv. Funct. Mater. 29 (2019) 1901721.
[22] Z. Lei, Q. Wang, S. Sun, W. Zhu, P. Wu, Adv. Mater. 29 (2017) 1700321.
[23] W. Kong, C. Wang, C. Jia, et al., Adv. Mater. 30 (2018) 1801934.
[24] L.W. Xia, R. Xie, X.J. Ju, et al., Nat. Commun. 4 (2013) 2226.
[25] S. Wei, W. Lu, X. Le, et al., Angew. Chem. Int. Ed. 58 (2019) 16243–16251.
[26] H. Shi, S. Wu, M. Si, et al., Adv. Mater. 34 (2022) 2107452.
[27] S. Wu, H. Shi, W. Lu, et al., Angew. Chem. Int. Ed. 60 (2021) 21890–21898.
[28] B. Wu, H. Lu, X. Le, et al., Chem. Sci. 12 (2021) 6472–6487.
[29] H. Liu, S. Wei, H. Qiu, et al., Adv. Funct. Mater. 32 (2022) 2108830.
[30] W. Lu, M. Si, H. Liu, et al., Cell Rep. Phys. Sci. 2 (2021) 100417.
[31] S. Wei, H. Qiu, H. Shi, et al., ACS Nano 15 (2021) 10415–10427.
[32] W. Lu, S. Wei, H. Shi, et al., Aggregate 2 (2021) e37.
[33] H. Qiu, S. Wei, H. Liu, et al., Adv. Intell. Syst. 3 (2021) 2000239.
[34] X. Le, H. Shang, H. Yan, et al., Angew. Chem. Int. Ed. 60 (2021) 3640–3646.
[35] S. Wei, Y. Li, W. Lu, et al., Angew. Chem. Int. Ed. 60 (2021) 8608–8624.
[36] J. Li, Z. Wang, H. Han, et al., Chin. Chem. Lett. 33 (2022) 1936–1940.
[37] H. Wang, C.N. Zhu, H. Zeng, et al., Adv. Mater. 31 (2019) 1807328.
[38] C.N. Zhu, T. Bai, H. Wang, et al., Adv. Mater. 33 (2021) 2102023.
[39] Q. Wang, Q. Wang, Acc. Chem. Res. 54 (2021) 1274–1287.
[40] Y. Miao, M. Xu, L. Zhang, Adv. Mater. 33 (2021) 2102308.
[41] J. Yin, W. Fan, Z. Xu, et al., Small 18 (2022) 2104440.
[42] X. Zhang, N. Sheng, L. Wang, et al., Mater. Horiz. 6 (2019) 326–333.
[43] B. Sui, Y. Li, B. Yang, Chin. Chem. Lett. 31 (2020) 1443–1447.
[44] H. Xu, B.W. Zeiger, K.S. Suslick, Chem. Soc. Rev. 42 (2013) 2555–2567.
[45] J. Luo, Z. Xie, J.W.Y. Lam, et al., Chem. Commun. (2001) 1740–1741.
[46] J. Mei, N.L.C. Leung, R.T.K. Kwok, J.W.Y. Lam, B.Z. Tang, Chem. Rev. 115 (2015) 11718–11940.
[47] Z. Guo, J. Zhao, Y. Liu, et al., Chin. Chem. Lett. 32 (2021) 1691–1695.
[48] C. Qin, Y. Li, Q. Li, C. Yan, L. Cao, Chin. Chem. Lett. 32 (2021) 3531–3534.
[49] R. Fu, L. Yu, J. Zhang, et al., Chin. Chem. Lett. 33 (2022) 1993–1996.
[50] G.Q. Yin, H. Wang, X.Q. Wang, et al., Nat. Commun. 9 (2018) 567.
[51] G.Q. Yin, S. Kandapal, C.H. Liu, et al., Angew. Chem. Int. Ed. 60 (2021) 1281–1289.
[52] X. Ma, W. Chi, X. Han, et al., Chin. Chem. Lett. 32 (2021) 1790–1794.
[53] N. Wang, H. Yao, Q. Tao, et al., Chin. Chem. Lett. 33 (2022) 252–256.
[54] T. Zhang, Y. Liu, B. Hu, et al., Chin. Chem. Lett. 30 (2019) 949–952.
[55] J. Guo, Y. Li, Y. Zhang, et al., ACS Appl. Mater. Interfaces 13 (2021) 40079–40087.
[56] N. Sabbatini, M. Guardigli, J.M. Lehn, Coord. Chem. Rev. 123 (1993) 201–228.